

Stress-driven nonlocal elasticity for nonlinear vibration characteristics of carbon/boron-nitride hetero-nanotube subject to magneto-thermal environment

Hamid M Sedighi^{1,2,4}  and Mohammad Malikan³ 

¹Mechanical Engineering Department, Faculty of Engineering, Shahid Chamran University of Ahvaz, Ahvaz, PO Box: 61357-43337, Iran

²Drilling Excellence and Research Center, Shahid Chamran University of Ahvaz, Ahvaz, Iran

³Department of Mechanics of Materials and Structures, Faculty of Civil and Environmental Engineering, Gdansk University of Technology, PO Box: 80-233, Gdansk, Poland

E-mail: h.msedighi@scu.ac.ir, hmsedighi@gmail.com, mohammad.malikan@yahoo.com and mohammad.malikan@pg.edu.pl

Received 26 November 2019, revised 22 February 2020

Accepted for publication 26 February 2020

Published 5 March 2020



CrossMark

Abstract

Stress-driven nonlocal theory of elasticity, in its differential form, is applied to investigate the nonlinear vibrational characteristics of a hetero-nanotube in magneto-thermal environment with the help of finite element method. In order to more precisely deal with the dynamic behavior of size-dependent nanotubes, a two-node beam element with six degrees-of freedom including the nodal values of the deflection, slope and curvature is introduced. In comparison with the conventional beam element, the vector of nodal displacement for the proposed element has one additional component indicating the nodal curvature to comply with the stress-driven nonlocal beam model. The nonlinear term associated with the von Kármán strain is included in the governing equation of motion and it is assumed that the nanotube structure is exposed to temperature changes and surrounded by a magnetic field. The obtained results endorsing the amplitude-dependence of the nonlinear frequencies are justified compared to those reported in the literature and a detailed study is conducted to explore the effect of different parameters on the vibrational behavior of the considered nano-hetero-structure.

Keywords: stress-driven nonlocal elasticity, hetero-nanotube, nonlinear finite element method, magnetic field, thermal environment

(Some figures may appear in colour only in the online journal)

1. Introduction

From structural point of view, boron-nitride nanotubes (BNNTs) are similar to their counterpart carbon nanotubes (CNTs), where boron and nitrogen atoms are replaced by carbon atoms. Nanotubes are pivotal building blocks in the modern photonic/electronic structures and systems thanks to good compatibility with different adaptive synthetic processes

and also their excellent optoelectronic features. Several inspiring investigations have been reported by applying these nanostructures in the fabrication of different kinds of nanoelectromechanical systems such as sensors and actuators, gas/pressure indicators, biomedical devices and etc [1–9].

Since their practical discovery in 1995, extensive researches have been focused on exploring mechanical, chemical and physical properties of boron-nitride nanotubes. In the meantime, scientists have just begun investigating the applications/advantages of such small-scale structures in

⁴ Author to whom any correspondence should be addressed.

high-tech electronic devices, nanomedicine and pharmacology, and recent findings have made them as one of the most amazing types of non-carbon nanotubes. To date, carbon nanotubes have been extensively exploited for medical purposes, but their inherent toxicity has limited their usage. Owing to the specific characteristics of boron-nitride nanotubes, such as chemical stability, superior mechanical and electronic properties, thermal conductivity and most importantly superb biocompatibility, more recently, scientific communities have been paying more attention to this kind of nanotubes. It is noted that a layered BNNT is more stable than a graphite carbon material when exposed to temperature gradients or chemical interactions [5, 10–15]. On the other hand, CNTs with their cylindrical geometry are allotropes of carbon. It is empirically demonstrated that they possess high thermal conductivity with extraordinary physio-mechanical properties. It should be emphasized that carbon and boron-nitride nanotubes have outstanding features due to their high surface area to volume ratio. Moreover, CNTs have chirality-dependent properties which makes them to behave as a semiconducting or metallic material depending on the rolling direction.

Although BNNTs are very similar to CNTs in the arrangement of atomic structure, only CNTs can behave as a metallic nano-structural tube with high conductivity [16, 17]. It can be certainly mentioned that hybridizing both nanotubes to have a new nano-hetero-structure may have more advantages than using them alone. Therefore, having a composite nanotube made from both aforementioned materials would be an inspiring idea which leads to a new class of nanostructures, namely C/BN hetero-nanotubes. C/BNNTs, as a new nanoscale materials, can be synthesized as a non-conventional supercapacitors which hybridize CNTs, as a conductive electrode, to BNNTs as a dielectric layer. Dielectric structures are those which can be polarized by an external electric voltage and capacitors are those that can be used as a high energy storage devices. The galvanized advantage of these supercapacitors in contrast to the traditional capacitors like batteries and fuel cells is indeed their less energy densities [18].

Motivated by these applications, Carbon/Boron-Nitride (C/BN) hetero-nanotubes can be synthesized to produce the next generation of smart/intelligent nano-devices such as nano sensors and actuators. Rodríguez Juárez *et al* [19] reported the mechanical, magnetic and electronic properties of different combinations of C-BNNTs and proposed them for utilizing in drug delivery systems as well as nano-vehicles. The transport features and conductance of a hetero-structure made up of carbon and boron-nitride nanotubes was investigated by Xiao *et al* [20]. In another work, on the basis of molecular dynamics simulations and continuum elasticity theory, the occurrence of beat phenomenon in analyzing the natural frequencies of a BN-CNT was reported by Zhang and Wang [21]. They emphasized that the essential difficulties in producing mass detectors for atomic-scale measuring may be resolved by interaction between two vibration modes of the hetero-nanotubes. Based on the non-equilibrium Green's function assumptions, a theoretical investigation on the

C-BN-C nanotubes was performed by Vedaai and Nadimi [22] where the tendency of NO_2 and O_2 molecules toward a chemical attachment with the surface of the hetero-nanotube was demonstrated. Within the framework of molecular mechanics theory, Chen *et al* [23] theoretically identified the prominent thermal rectification impacts of a rectifier-based C/BN nanotube and investigated the thermal transport across its interface. Moreover, it was demonstrated that when the system is subjected to a high temperature bias, the armchair hetero-nanotubes have less thermal rectification (TR) ratio than that of zigzag C/BN ones. With the aid of molecular dynamics (MD) simulations, Badjian and Setoodeh [24] utilized a boron nitride nanotube to coat a defected carbon nanotube and enhanced the tensile and buckling behavior of the homogenous nanotube. They demonstrated that while atom vacancies considerably affect the buckling behavior of CNTs, the presence of BNNT coating result in improving the mechanical strength of such nanotubes. On the basis of Morse and cosine potential functions, Genoese *et al* [25] analyzed the nanoscale behavior of single-walled silicon carbide (SiC), boron-nitride (BN) and carbon (C) nanotubes using molecular dynamics. Both armchair and zigzag patterns were considered and the elastic properties of the studied nanotubes were evaluated by means of Donnell thin shell theory. With the aid of MD simulations, the modal participation of a doubly-clamped single-walled CNTs in the presence of vacancies was studied by Eltaher *et al* [26]. Kiani *et al* [27] investigated the free vibration behavior of single-layered of double-walled carbon nanotubes (DWCNTs) by means of constitutive non-local theories. They employed the nonlocal Timoshenko and Rayleigh beam models to extract the governing equations of motion and evaluated the nonlocal natural frequencies of the considered structure. The nonlocal natural frequencies of a hinged-hinged hybrid nanotube were studied by Cheng *et al* [19]. They found the numerical solution of the harvested equations by means of dynamic stiffness technique and exhibited that the considered nanotube becomes more unstable at larger values of nonlocal and length ratio parameters. A great deal of research works has been recently conducted in the case of hybrid/homogeneous nanostructures which are not reported here, for the sake of brevity [28–40].

The vibration characteristics of nanostructures are of great importance, not only in linear modes but also in non-linear states, in light of the nonlinear effects which physically stem from the flexibility of such structures. As far as the electronic/magnetic nano-devices are fabricated from CNTs and BNNTs segments, a detailed knowledge about their nonlinear behavior is necessary that was an incentive idea for the authors to perform this theoretical research. Therefore, the present study deals with the nonlinear vibrational behavior of a carbon/boron-nitride hetero-nanotube employing nonlinear finite element method. A two-node beam-like element with six degrees of freedom is introduced to more accurately capture the size-dependent behavior of nanotubes. To formulate the nanoscale aspects of such structures, nonlocal elasticity theories in the context of strain- and stress-driven frameworks, can be utilized [41–45]. In this research, however, the stress-driven approach is considered in the

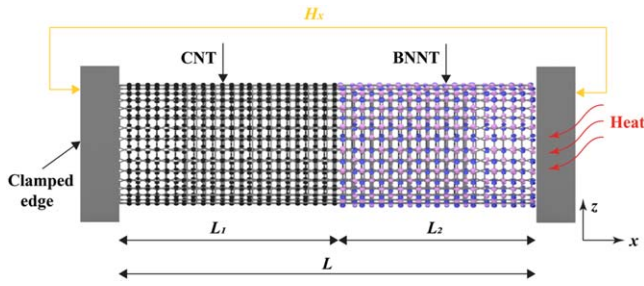


Figure 1. The schematic configuration of the hybrid nanotube made of CNT and BNNT.

constitutive equations. It is assumed that the magneto-thermal environment surrounds the hetero-nanotube and the effects of nonlocality, initial amplitude and length ratio parameter are investigated here through a nonlinear finite element analysis. The obtained results, for some special cases, are justified in comparison with those reported in the literature.

2. Mathematical formulation

In this section, the nonlocal differential equation governs the nonlinear vibrational behavior of a hetero-nanotube is extracted. The mentioned hetero-nanotube is synthesized using boron-nitride and carbon nanotube segments in which two parts are assumed to have similar cylindrical geometries and different thermal/mechanical properties. As shown in figure 1, the entire nanotube length is denoted by L in which the first fragment is composed of carbon material with the length of $L_1 = \xi L$ ($0 < \xi < 1$). The nano-hetero-structure with doubly-clamped end conditions is surrounded by an axial magnetic field H_x and considered to be exposed to temperature changes.

2.1. Stress-driven nonlocal theory of elasticity

In order to describe the nanoscale behavior of the hetero-nanotube, the stress-driven nonlocal model is adopted here. Compared to the conventional strain-driven approaches, in the stress-driven model of nonlocal elasticity, the strain vector in each point of the elastic medium is assumed to be a function of the overall stress vector given by the following integral from [46–50]:

$$\varepsilon(x) = \int_V \varphi_\lambda(x, \bar{x}) C(\bar{x}) : \sigma(\bar{x}) d\bar{x} \quad (1)$$

in which $\varphi_\lambda(x, \bar{x})$ represents the kernel attenuation function and C denotes the elastic compliance matrix. It is noted that with this kind of definition, one can readily find the analytical response of the problem in a convenient way. To this end, the only valid components of strain and stress for a beam-like nanotube in the longitudinal direction can be described by the following nonlocal stress-strain relationship as:

$$\varepsilon(x) = \frac{1}{EI} \int_0^L \varphi_\lambda(x - \bar{x}) \sigma(\bar{x}) d\bar{x} \quad (2)$$

On the other hand, by considering the bending problem and manipulating the above-mentioned equation, the relationship between the curvature and moment of the nanotube is given as follows:

$$\chi(x) = \frac{1}{EI} \int_0^L \varphi_\lambda(x - \bar{x}) M(\bar{x}) d\bar{x} \quad (3)$$

In order to facilitate the application of the proposed approach, it is convenient to introduce the differential form of equation (3) by describing the kernel function $\varphi_\lambda(x, \bar{x})$ using a bi-exponential function as follows:

$$\varphi_\lambda(x, \bar{x}) = \frac{1}{2L_c} \exp\left(-\frac{|x - \bar{x}|}{L_c}\right) \quad (4)$$

where L_c is the characteristic length of nanotube and the nonlocal parameter is defined by $\lambda = L_c/L$. Therefore, one can obtain the differential form of the stress-driven nonlocal elasticity as:

$$\chi''(x) - \frac{1}{L_c^2} \chi(x) = -\frac{1}{EIL_c^2} M(x) \quad (5)$$

together with the following boundary conditions:

$$BC \begin{cases} \chi'(0) = \frac{1}{L_c^2} \chi(0) \\ \chi'(L) = \frac{1}{L_c^2} \chi(L) \end{cases} \quad (6)$$

The above-mentioned stress-driven formulation is exploited to derive the governing equation for vibrating hybrid-nanotube in the magnetic-thermal environment.

2.2. Lorentz force

In order to obtain the Lorentz force formulation in the presence of axial magnetic field, we consider the differential form of Maxwell's equations. In the case of conducting elastic material, the Maxwell's relations are written as follows [36]:

$$\mathbf{J} = \nabla \times \mathbf{h} \quad (7)$$

$$\nabla \times \mathbf{E} = -\mu \frac{\partial \mathbf{h}}{\partial t} \quad (8)$$

$$\nabla \cdot \mathbf{h} = 0 \quad (9)$$

$$\mathbf{E} = -\mu \left(\frac{\partial \mathbf{U}}{\partial t} \times \mathbf{H} \right) \quad (10)$$

$$\mathbf{h} = \nabla \times (\mathbf{U} \times \mathbf{H}) \quad (11)$$

in which \mathbf{J} , \mathbf{h} , \mathbf{E} and \mathbf{U} represent the current density, the disturbing vectors of magnetic field, the strength vectors of electric field and the displacement vector, respectively. Moreover, in the above equations, $\nabla = \frac{\partial}{\partial x} \hat{e}_x + \frac{\partial}{\partial y} \hat{e}_y + \frac{\partial}{\partial z} \hat{e}_z$ is the Hamilton differential operator and μ denotes the magnetic field permeability. Applying the longitudinal magnetic field $\mathbf{H} = (H_x, 0, 0)$ and considering the displacement vector as $\mathbf{U} = (0, v, w)$, the current density and the disturbing vectors of magnetic field are written by:

$$\mathbf{h} = \nabla \times (\mathbf{U} \times \mathbf{H}) = -H_x \left(\frac{\partial v}{\partial y} + \frac{\partial w}{\partial z} \right) \hat{\mathbf{e}}_x + H_x \frac{\partial v}{\partial x} \hat{\mathbf{e}}_y + H_x \frac{\partial w}{\partial x} \hat{\mathbf{e}}_z \tag{12}$$

$$\mathbf{J} = \nabla \times \mathbf{h} = -H_x \left(\frac{\partial^2 v}{\partial x \partial z} - \frac{\partial^2 w}{\partial x \partial y} \right) \hat{\mathbf{e}}_x - H_x \times \left(\frac{\partial^2 v}{\partial y \partial z} + \frac{\partial^2 w}{\partial x^2} + \frac{\partial^2 w}{\partial z^2} \right) \hat{\mathbf{e}}_y + H_x \left(\frac{\partial^2 v}{\partial x^2} + \frac{\partial^2 v}{\partial y^2} + \frac{\partial^2 w}{\partial y \partial z} \right) \hat{\mathbf{e}}_z \tag{13}$$

Thereby, the Lorentz force denoted by F_L (a body force) induced by the longitudinal magnetic field can be achieved as:

$$\mathbf{F}_L = \mu (\mathbf{J} \times \mathbf{H}) = \mu H_x^2 \left[\left(\frac{\partial^2 v}{\partial x^2} + \frac{\partial^2 v}{\partial y^2} + \frac{\partial^2 w}{\partial y \partial z} \right) \hat{\mathbf{e}}_y + \left(\frac{\partial^2 w}{\partial x^2} + \frac{\partial^2 w}{\partial y^2} + \frac{\partial^2 v}{\partial y \partial z} \right) \hat{\mathbf{e}}_z \right] \tag{14}$$

Since the current problem is assumed to be axisymmetric and the lateral displacement of C-BN nanotube is considered to be $w = w(x, t)$, the Lorentz force per unit length of the hybrid nanotube and in the z direction can be obtained as:

$$F_L = F_{zL} \hat{\mathbf{e}}_z = \mu A H_x^2 \frac{\partial^2 w}{\partial x^2} \hat{\mathbf{e}}_z \tag{15}$$

where A represents the nanotube cross section area.

2.3. Elastic-beam model with temperature changes and von-kármán nonlinearity

In the current work, the Euler–Bernoulli beam model, which is efficiently used to study the nonlinear vibrational behavior of nanotubes, is adopted to develop the governing equations of motion for C-BN nanotube. To extract the governing equation of motion, we consider a straight hetero-nanotube under bending with length L and cross-section A . The longitudinal axis of nanotube coincides with the x axis. The displacement field of the classical beam theory is written by:

$$u_1(x, z, t) = u(x, t) - z \frac{\partial w(x, t)}{\partial x} \tag{16a}$$

$$u_3(x, z, t) = w(x, t) \tag{16b}$$

where the meaningful displacements of each point are represented by $u_i (i = 1, 3)$ in x and z directions, respectively. In this work, in-plane components of displacement vector in the axial and transverse directions are denoted by u and w , respectively in which the axis z shows the coordinate through the thickness of the nanotube. To consider the geometric nonlinearity of the structure and also the thermo-elastic axial strain, the following form of Lagrangian strains are adopted as:

$$\epsilon_{xx} = \frac{\partial u}{\partial x} - z \frac{\partial^2 w}{\partial x^2} + \frac{1}{2} \left(\frac{\partial w}{\partial x} \right)^2 - \alpha_x \Delta T \tag{17}$$

in which α_x depicts the thermal expansion coefficient along x axis and ΔT displays the temperature changes. The Hamilton’s principle is utilized here to develop the governing equations. Therefore, one can write:

$$\int_{t_1}^{t_2} (\Pi_W - \Pi_U + \Pi_K) dt = 0 \tag{18}$$

where Π_U and Π_W denote the strain energy and work done by the external forces and Π_K represents the Kinetic energy. Considering equation (17), the variational form of the strain energy can be written as:

$$\delta \Pi_U = \int_V (\sigma_{xx} \delta \epsilon_{xx}) dV \tag{19}$$

By performing some calculations, the non-classical boundary conditions as well as the equilibrium equation can be expressed as:

$$\delta \Pi_{U_{\text{Equilibrium equation}}} = - \int_0^L \left(\frac{\partial N_{xx}}{\partial x} \delta u + \frac{\partial^2 M_{xx}}{\partial x^2} \delta w \right) dx \tag{20}$$

$$\delta \Pi_{U_{\text{Boundary conditions}}} = \left(N_{xx} \delta u - M_{xx} \frac{\partial \delta w}{\partial x} + \frac{\partial M_{xx}}{\partial x} \delta w \right) \Big|_0^L \tag{21}$$

in which

$$N_x = \int_{-h/2}^{h/2} \sigma_{xx} dz \tag{22}$$

$$M_x = \int_{-h/2}^{h/2} \sigma_{xx} z dz \tag{23}$$

The work done by the non-conservative axial force N_x is given by:

$$\Pi_W = \frac{1}{2} \int_0^L N_x \left(\frac{\partial w}{\partial x} \right)^2 dx \tag{24}$$

and in the variational form can be written as:

$$\delta \Pi_W = \int_0^L N_x \left(\frac{\partial \delta w}{\partial x} \frac{\partial w}{\partial x} \right) dx \tag{25}$$

It should be pointed out that the in-plane axial force N_x is assumed to include both contributions of magneto-thermal environment. On the other hand, the kinetic energy is expressed by:

$$\Pi_K = \frac{1}{2} \int \int_A \rho(z) \left[\left(\frac{\partial u_1}{\partial t} \right)^2 + \left(\frac{\partial u_3}{\partial t} \right)^2 \right] dA dz \tag{26}$$

The variational form of kinetic energy can be concluded as:

$$\delta \Pi_K = \int_A \left(I_m \frac{\partial^4 w}{\partial x^2 \partial t^2} \delta w - m \frac{\partial^2 w}{\partial t^2} \delta w \right) dA \tag{27}$$

in which m is the nanotube mass per unit length and I_m is the second mass moment of inertia described by the following relations:

$$(m, I_m) = \int_{-h/2}^{h/2} \rho(z) (1, z^2) dz \tag{28}$$

where ρ represents the mass density of nanotube. In this paper, the effect of second mass moment of inertia I_m is neglected.

Thereafter, by applying equation (18) and considering the adjacent equilibrium method, one can obtain the governing equations of the present problem as:

$$-\frac{\partial^2 M_x}{\partial x^2} + N_x \frac{\partial^2 w}{\partial x^2} = m \frac{\partial^2 w}{\partial t^2} \quad (29)$$

To examine the effect of in-plane stretching, the following equation should be considered:

$$N_x = EA \left[\frac{\partial u}{\partial x} + \frac{1}{2} \left(\frac{\partial w}{\partial x} \right)^2 \right] = C_1 = cte \quad (30)$$

in which the parameter C_1 is calculated by integrating equation (30). One can find:

$$EA[u(L) - u(0)] + \frac{EA}{2} \int_0^L \left(\frac{\partial w}{\partial x} \right)^2 dx = C_1 L \quad (31)$$

Thereby, considering the end conditions $u(0) = u(L) = 0$ and rearranging the above-mentioned equation leads to:

$$C_1 = N_x = \frac{1}{2} \frac{EA}{L} \int_0^L \left(\frac{\partial w}{\partial x} \right)^2 dx \quad (32)$$

Furthermore, based upon the thermal elasticity theory, the axial load N_t denoting the effect of thermal gradients is expressed as:

$$N_t = -\frac{EA}{1 - 2\nu} \alpha_x \Delta T \quad (33)$$

where ν symbolizes the Poisson's ratio of nanotube. Taking into account the effect of magneto-thermal environment, the equation of motion governing the dynamic behavior of nanotube is re-formulated as:

$$\begin{aligned} \frac{\partial^2 M}{\partial x^2} = & -m \frac{\partial^2 w}{\partial t^2} + \left(\frac{1}{2} \frac{EA}{L} \int_0^L \left(\frac{\partial w}{\partial x} \right)^2 dx \right) \frac{\partial^2 w}{\partial x^2} \\ & + N_t \frac{\partial^2 w}{\partial x^2} + F_{zL} \end{aligned} \quad (34)$$

with the following boundary conditions:

$$w(0, t) = w(L, t) = \frac{\partial w(0, t)}{\partial x} = \frac{\partial w(L, t)}{\partial x} = 0 \quad (35)$$

2.4. Governing equations of motion for C/BN hetero-nanotube

According to the Bernoulli-Euler beam theory, by ignoring the nonlinear terms, the curvature-deflection relation for a given point of nanotube is expressed by:

$$\chi(x) = \frac{\partial^2 w}{\partial x^2} \quad (36)$$

In order to develop the dynamic equation of motion, the second derivative of equation (5) with respect to x are represented as:

$$\frac{\partial^4 \chi(x)}{\partial x^4} - \frac{1}{L_c^2} \frac{\partial^2 \chi(x)}{\partial x^2} = -\frac{1}{EIL_c^2} \frac{\partial^2 M(x)}{\partial x^2} \quad (37)$$

Thereby, by considering equations (34) and (36), the governing equation for the stress-driven vibrating nanotube in the presence of magneto-thermal environment can be extracted as follows:

$$\begin{aligned} EIL_c^2 \frac{\partial^6 w}{\partial x^6} - EI \frac{\partial^4 w}{\partial x^4} = & m \frac{\partial^2 w}{\partial t^2} - \left(\frac{1}{2} \frac{EA}{L} \int_0^L \left(\frac{\partial w}{\partial x} \right)^2 dx \right) \\ & \times \frac{\partial^2 w}{\partial x^2} + \frac{EA\alpha_x \Delta T}{1 - 2\nu} \frac{\partial^2 w}{\partial x^2} - \mu AH_x^2 \frac{\partial^2 w}{\partial x^2} \end{aligned} \quad (38)$$

Equation (25) governs the motion of two parts of hetero-nanotube. Representing the subscripts 'C' and 'BN' for carbon and boron-nitride fragments results in:

$$\begin{aligned} E_C I L_c^2 \frac{\partial^6 w}{\partial x^6} = & E_C I \frac{\partial^4 w}{\partial x^4} + m_C \frac{\partial^2 w}{\partial t^2} - \left(\frac{1}{2} \frac{E_C A}{L} \right. \\ & \times \left. \int_0^L \left(\frac{\partial w}{\partial x} \right)^2 dx \right) \frac{\partial^2 w}{\partial x^2} + \frac{E_C A \alpha_{xC} \Delta T}{1 - 2\nu} \frac{\partial^2 w}{\partial x^2} \\ & - \mu A H_x^2 \frac{\partial^2 w}{\partial x^2} \quad \text{for } 0 \leq x < \xi L \end{aligned} \quad (39)$$

$$\begin{aligned} E_{BN} I L_c^2 \frac{\partial^6 w}{\partial x^6} = & E_{BN} I \frac{\partial^4 w}{\partial x^4} + m_{BN} \frac{\partial^2 w}{\partial t^2} \\ & - \left(\frac{1}{2} \frac{E_{BN} A}{L} \int_0^L \left(\frac{\partial w}{\partial x} \right)^2 dx \right) \frac{\partial^2 w}{\partial x^2} + \frac{E_{BN} A \alpha_{xBN} \Delta T}{1 - 2\nu} \\ & \times \frac{\partial^2 w}{\partial x^2} - \mu A H_x^2 \frac{\partial^2 w}{\partial x^2} \quad \text{for } \xi L \leq x < L \end{aligned} \quad (40)$$

The following dimensionless parameters are defined to describe the governing equations in non-dimensional form:

$$\begin{aligned} \bar{x} = \frac{x}{L}, W_i = \frac{w_i}{L}, \tau = t \sqrt{\frac{E_C I}{m_C L^4}}, e_n = \frac{L_c}{L}, \\ \alpha_1 = \frac{E_{BN}}{E_C}, \alpha_2 = \frac{m_{BN}}{m_C}, \bar{\alpha}_{xC} = \frac{\alpha_{xC} \Delta T L^2}{1 - 2\nu r^2}, \\ \bar{\alpha}_{xBN} = \frac{\alpha_{xBN} \Delta T L^2}{1 - 2\nu r^2}, h_x = \frac{\mu A H_x^2 L^2}{E_C I}, \end{aligned} \quad (41)$$

in which r is the radius of gyration of the nanotube. By using the above-mentioned parameters, the non-dimensional form of the nonlinear equations of motion for two segments of hetero-nanotube are given by:

$$\begin{aligned} -e_n^2 \frac{\partial^6 W_1}{\partial \bar{x}^6} + \frac{\partial^4 W_1}{\partial \bar{x}^4} + \frac{\partial^2 W_1}{\partial \tau^2} - \left(\frac{1}{2} \int_0^L \left(\frac{\partial W}{\partial \bar{x}} \right)^2 dx \right) \frac{\partial^2 W_1}{\partial \bar{x}^2} \\ + \bar{\alpha}_{xC} \frac{\partial^2 W_1}{\partial \bar{x}^2} - h_x \frac{\partial^2 W_1}{\partial \bar{x}^2} = 0, \\ \text{for } 0 \leq \bar{x} < \xi \end{aligned} \quad (42)$$

$$\begin{aligned}
 & -\alpha_1 e_n^2 \frac{\partial^6 W_2}{\partial \bar{x}^6} + \alpha_1 \frac{\partial^4 W_2}{\partial \bar{x}^4} + \alpha_2 \frac{\partial^2 W_2}{\partial \tau^2} - \left(\frac{\alpha_1}{2} \int_0^L \left(\frac{\partial W}{\partial \bar{x}} \right)^2 dx \right) \\
 & \times \frac{\partial^2 W_2}{\partial \bar{x}^2} + \alpha_1 \bar{\alpha}_{xBN} \frac{\partial^2 W_2}{\partial \bar{x}^2} - h_x \frac{\partial^2 W_2}{\partial \bar{x}^2} = 0, \\
 & \text{for } \xi \leq \bar{x} \leq 1
 \end{aligned} \tag{43}$$

subject to the following boundary/continuity conditions:

$$\begin{aligned}
 W_1(0, \tau) = W_2(1, \tau) = \frac{\partial W_1(0, \tau)}{\partial \bar{x}} = \frac{\partial W_2(1, \tau)}{\partial \bar{x}} = 0, \\
 \text{essential boundary conditions}
 \end{aligned} \tag{44}$$

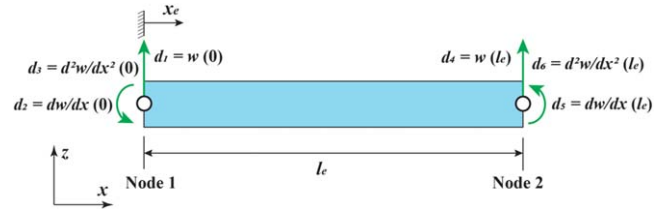


Figure 2. Beam element with six degrees of freedom.

displacement components includes the nodal values of the deflection and slope. The schematic configuration of the nonlocal beam element is illustrated in figure 2. The following polynomial displacement function of degree 5 is adopted

$$\left. \begin{aligned}
 & W_1(\bar{x}, \tau)|_{\bar{x}=\xi} = W_2(\bar{x}, \tau)|_{\bar{x}=\xi} \\
 & \left. \frac{\partial W_1(\bar{x}, \tau)}{\partial \bar{x}} \right|_{\bar{x}=\xi} = \left. \frac{\partial W_2(\bar{x}, \tau)}{\partial \bar{x}} \right|_{\bar{x}=\xi} \\
 & e_n^2 \left. \frac{\partial^4 W_1(\bar{x}, \tau)}{\partial \bar{x}^4} \right|_{\bar{x}=\xi} - \left. \frac{\partial^2 W_1(\bar{x}, \tau)}{\partial \bar{x}^2} \right|_{\bar{x}=\xi} = \alpha_1 e_n^2 \left. \frac{\partial^4 W_2(\bar{x}, \tau)}{\partial \bar{x}^4} \right|_{\bar{x}=\xi} - \alpha_1 \left. \frac{\partial^2 W_2(\bar{x}, \tau)}{\partial \bar{x}^2} \right|_{\bar{x}=\xi} \\
 & e_n^2 \left. \frac{\partial^5 W_1(\bar{x}, \tau)}{\partial \bar{x}^5} \right|_{\bar{x}=\xi} - \left. \frac{\partial^3 W_1(\bar{x}, \tau)}{\partial \bar{x}^3} \right|_{\bar{x}=\xi} = \alpha_1 e_n^2 \left. \frac{\partial^5 W_2(\bar{x}, \tau)}{\partial \bar{x}^5} \right|_{\bar{x}=\xi} - \alpha_1 \left. \frac{\partial^3 W_2(\bar{x}, \tau)}{\partial \bar{x}^3} \right|_{\bar{x}=\xi}
 \end{aligned} \right\} \text{continuity conditions at the junction of } \bar{x} = \xi \tag{45}$$

Equations (42) and (43) together with the boundary conditions (44) and (45) are then solved with the help of a nonlinear finite element method.

3. Solution methodology

The dynamic equation of motion for C/BN hybrid nanotube in the presence of magneto-thermal environment is given by equations (42) and (43) subject to the boundary/continuity conditions in equations (44) and (45). A nonlinear finite element method is exploited to decompose the governing equations. In view of the stress-driven nonlocal nanotube and in order to more accurately predict the size-dependent behavior, a two-node beam-like element with six degrees of freedom is presented. Therefore, for a nonlocal beam element, it is necessary to prescribe three degrees of freedom, i.e. the deflection, slope and curvature at each node. Hence, the nodal displacement components for this kind of beam element can be defined as:

$$\begin{aligned}
 d_1^e = W(\bar{x}_e = 0), d_2^e = \left. \frac{\partial W}{\partial \bar{x}} \right|_{\bar{x}_e=0}, d_3^e = \left. \frac{\partial^2 W}{\partial \bar{x}^2} \right|_{\bar{x}_e=0}, \\
 d_4^e = W(\bar{x}_e = l_e), d_5^e = \left. \frac{\partial W}{\partial \bar{x}} \right|_{\bar{x}_e=l_e}, d_6^e = \left. \frac{\partial^2 W}{\partial \bar{x}^2} \right|_{\bar{x}_e=l_e}
 \end{aligned} \tag{46}$$

in which l_e is the length of beam element. It should be pointed out that for the conventional beam element, the nodal

for the nanotube elements:

$$W_e(\bar{x}) = a_1 + a_2 \bar{x} + a_3 \bar{x}^2 + a_4 \bar{x}^3 + a_5 \bar{x}^4 + a_6 \bar{x}^5 \tag{47}$$

and the element nodal displacements at two nodes are defined by:

$$\{d_e\}^T = [d_1^e \ d_2^e \ d_3^e \ d_4^e \ d_5^e \ d_6^e] \tag{48}$$

The displacement field as a function of shape functions N_i can be written as:

$$W_e(\bar{x}) = [N_1 \ N_2 \ N_3 \ N_4 \ N_5 \ N_6] \{d_e\} \tag{49}$$

where

$$\begin{aligned}
 N_1 &= \frac{-6\bar{x}_e^5 + 15\bar{x}_e^4 l_e - 10\bar{x}_e^3 l_e^2 + l_e^5}{l_e^5}, \\
 N_2 &= \frac{-3\bar{x}_e^5 + 8\bar{x}_e^4 l_e - 6\bar{x}_e^3 l_e^2 + \bar{x}_e l_e^4}{l_e^4}, \\
 N_3 &= \frac{-\bar{x}_e^5 + 3\bar{x}_e^4 l_e - 3\bar{x}_e^3 l_e^2 + \bar{x}_e^2 l_e^3}{2l_e^3}, \\
 N_4 &= \frac{6\bar{x}_e^5 - 15\bar{x}_e^4 l_e + 10\bar{x}_e^3 l_e^2}{l_e^5}, \\
 N_5 &= \frac{-3\bar{x}_e^5 + 7\bar{x}_e^4 l_e - 4\bar{x}_e^3 l_e^2}{l_e^4}, \\
 N_6 &= \frac{\bar{x}_e^5 - 2\bar{x}_e^4 l_e + \bar{x}_e^3 l_e^2}{2l_e^3}
 \end{aligned} \tag{50}$$

Table 1. Comparison between the nonlinear natural frequency results of the clamped-clamped homogeneous beam for different theories.

W_{\max}/r	$(\omega_{NL}/\omega_L)^2$			Present work
	Generalized Finite Element Method [51]	Reduced GFEM [51]	Assumed Space Mode [52]	
0.1	1.0006	1.0006	1.0006	1.0006
0.2	1.0024	1.0024	1.0024	1.0024
0.4	1.0096	1.0096	1.0096	1.0096
0.6	1.0216	1.0216	1.0216	1.0216
0.8	1.0383	1.0384	1.0384	1.0383
1	1.0598	1.0599	1.0600	1.0598
1.5	1.1343	1.1349	1.1349	1.1343
2	1.2381	1.2398	1.2398	1.2382
3	1.5319	1.5395	1.5396	1.5320
4	1.9376	1.9591	1.9592	1.9377
5	2.4520	2.4986	2.4988	2.4522

The Galerkin weighted residuals method (GWRM) with the interpolation function N_i (as the weight function) can then be applied on equations (42) and (43). By assuming the solution of the problem in the following form:

$$W_i(\bar{x}, \tau) = W_e^i(\bar{x}) \exp(\lambda\tau), \quad i = 1, 2 \quad (51)$$

and using the GWRM weak form of the nonlinear equations of motion, one can obtain that:

$$[M]_e^C \ddot{W}_1 + [K]_e^C W_1 - N_C [K_{NL}]_e^C W_1 = 0 \quad (52)$$

$$[M]_e^{BN} \ddot{W}_2 + [K]_e^{BN} W_2 - N_{BN} [K_{NL}]_e^{BN} W_2 = 0 \quad (53)$$

where $[K_{NL}]_e^C$ and $[K_{NL}]_e^{BN}$ are the nonlinear stiffness matrices of the governing equations for carbon and boron-nitride nanotubes and we have:

$$\begin{aligned} [M]_e^C &= \int_0^{l_e} N^T N \, d\bar{x} \\ [K]_e^C &= -e_n^2 \int_0^{l_e} (N''')^T N''' \, d\bar{x} + \int_0^{l_e} (N'')^T N'' \, d\bar{x} \\ &\quad - \bar{\alpha}_{xC} \int_0^{l_e} (N')^T N' \, d\bar{x} + h_x \int_0^{l_e} (N')^T N' \, d\bar{x} \\ [K_{NL}]_e^C &= \int_0^{l_e} (N')^T N' \, d\bar{x} \end{aligned} \quad (54)$$

$$\begin{aligned} [M]_e^{BN} &= \alpha_2 \int_0^{l_e} N^T N \, d\bar{x} \\ [K]_e^{BN} &= -\alpha_1 e_n^2 \int_0^{l_e} (N''')^T N''' \, d\bar{x} + \alpha_1 \int_0^{l_e} (N'')^T N'' \, d\bar{x} \\ &\quad - \alpha_1 \bar{\alpha}_{xBN} \int_0^{l_e} (N')^T N' \, d\bar{x} + h_x \int_0^{l_e} (N')^T N' \, d\bar{x} \\ [K_{NL}]_e^{BN} &= \int_0^{l_e} (N')^T N' \, d\bar{x} \end{aligned} \quad (55)$$

Table 2. Properties of CNT and BNNT sections of hybrid nanotube.

Properties [53]	CNT	BNNT
Young's modulus (E) (TPa)	1	1.8
Density (ρ) (g cm ⁻³)	2.3	2.18
Outer Radius (nm)	3.5	3.5
Aspect ratio (L/2R _{out})	100	100
Thickness (h) (nm)	0.34	0.34
Coefficient of Thermal Expansion (Room Temperature) (K ⁻¹)	-1.6×10^{-6}	-0.3×10^{-6}
Coefficient of Thermal Expansion (High Temperature) (K ⁻¹)	1.1×10^{-6}	0.2×10^{-6}

In which the matrices $[K]$ represent stiffness and $[M]$ displays mass matrices, respectively. After applying the boundary/continuity conditions, using the assumed solution and performing the usual assemblage process, the characteristic equation for the hybrid C/BN nanotube is extracted as:

$$(\omega^2 [M] + [K] + N [K_{NL}]) \{\Delta_e\} = 0 \quad (56)$$

where ω are the eigenvalues and Δ_e are the eigenvectors of the hybrid nanotube and the nondimensional axial force N can be computed as:

$$\begin{aligned} N &= N_C + N_{BN} = \frac{1}{2} \sum_{i=1}^{n_C} \int_0^{l_e} W_{1,\bar{x}}^2 \, d\bar{x} + \frac{\alpha_1}{2} \sum_{i=1}^{n_{BN}} \int_0^{l_e} W_{2,\bar{x}}^2 \, d\bar{x} \\ &= \frac{1}{2} \{\Delta_e\}^T [K_{NL}]^C \{\Delta_e\} + \frac{\alpha_1}{2} \{\Delta_e\}^T [K_{NL}]^{BN} \{\Delta_e\} \end{aligned} \quad (57)$$

To solve the nonlinear eigenvalue problem described in equation (56), one can try to compute the exact nonlinear mode shape and the value of nonlinear frequency ω_{NL} corresponding to this mode is then calculated. Initial amplitude of vibration is selected, here we assume that the initial amplitude of the hybrid nanotube is the first mode shape of the linear system, and then the linear mode shape should be normalized to attain the maximum desired amplitude W_{\max} . Thereby, the nonlinear stiffness matrix for the whole nanotube $[K_{NL}]$ is calculated. The linearized eigenvalue problem leads to a modified nonlinear mode shape Δ_e as well as the corresponding nonlinear frequency ω_{NL} . The obtained mode shape should be normalized to get the desired maximum amplitude of the hybrid nanotube and this strategy is repeated until the selected convergence criterion is satisfied.

4. Results and discussion

4.1. Validation of the present analysis

To the best knowledge of the authors of this article, no research work in the literature has been yet conducted on the nonlinear vibrational characteristics of a clamped-clamped C/BN hetero-nanotube in the presence magnetic field and thermal gradients. Therefore, in order to justify the current analysis, table 1 presents the nonlinear frequencies of a

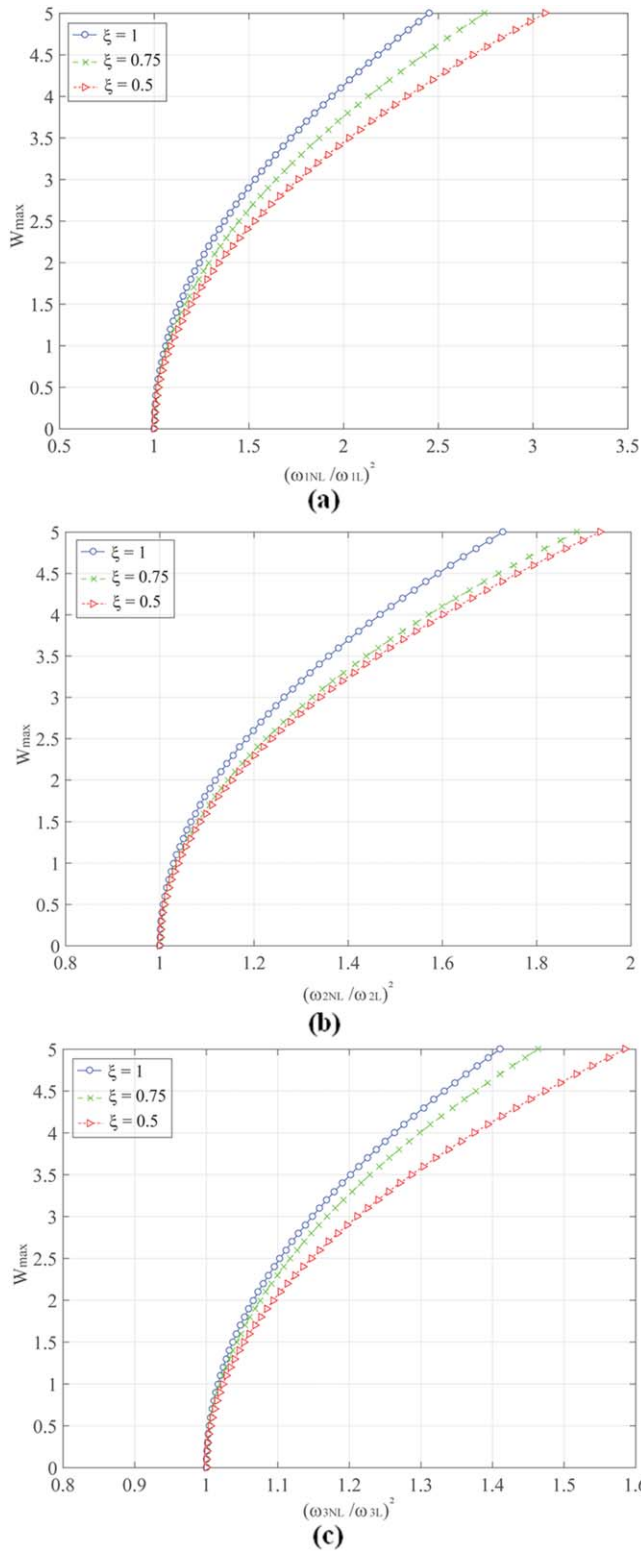


Figure 3. The effect of length ratio ξ on the dimensionless nonlinear to linear frequency ratio versus the maximum initial deflection of hybrid nanotube for ($h_x = 0, \Delta T = 0, e_n = 0, nu = 0.3, Rout = 3.5e-9, ht = 0.34e-9$) (a) first mode (b) second mode (c) third mode.

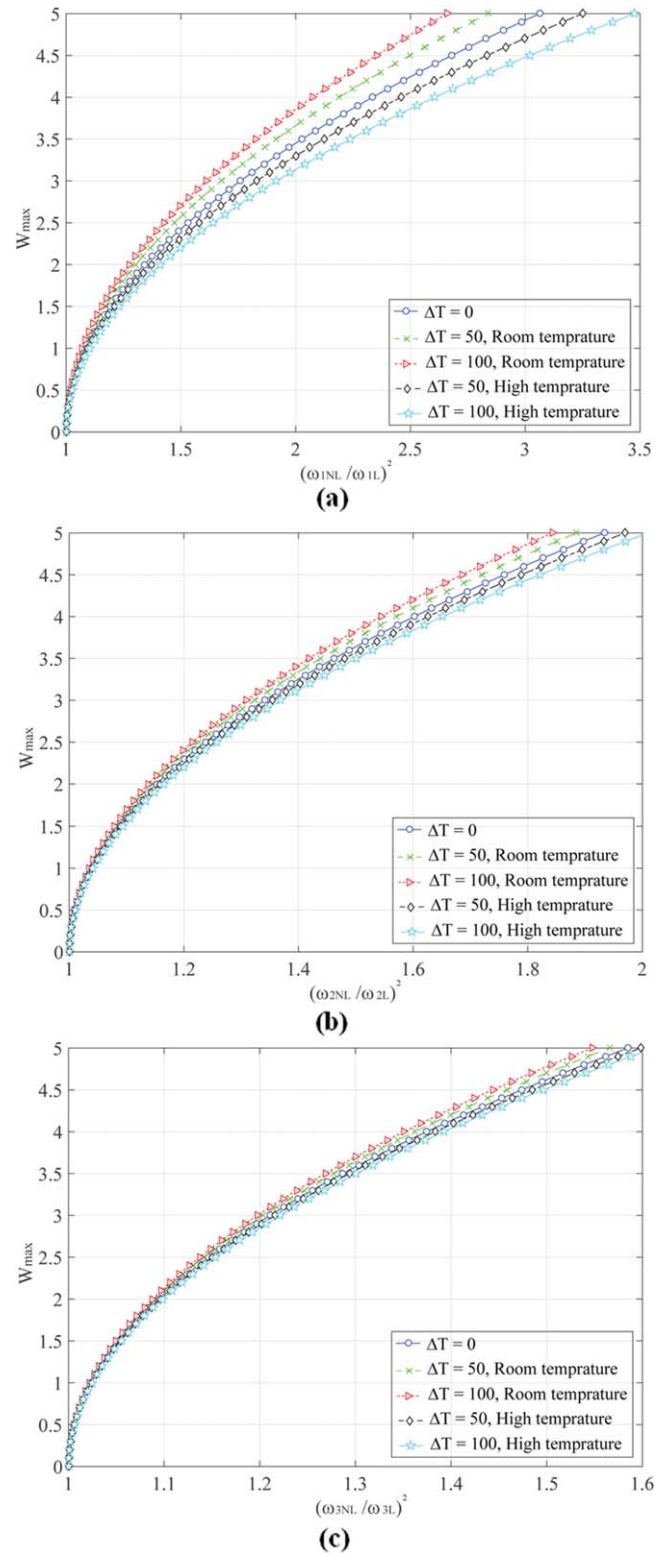


Figure 4. The effect of temperature change ΔT on the dimensionless nonlinear to linear frequency ratio versus the maximum initial deflection of hybrid nanotube for ($h_x = 0, \xi = 0.5, e_n = 0, nu = 0.3, Rout = 3.5e-9, ht = 0.34e-9$) (a) first mode (b) second mode (c) third mode.

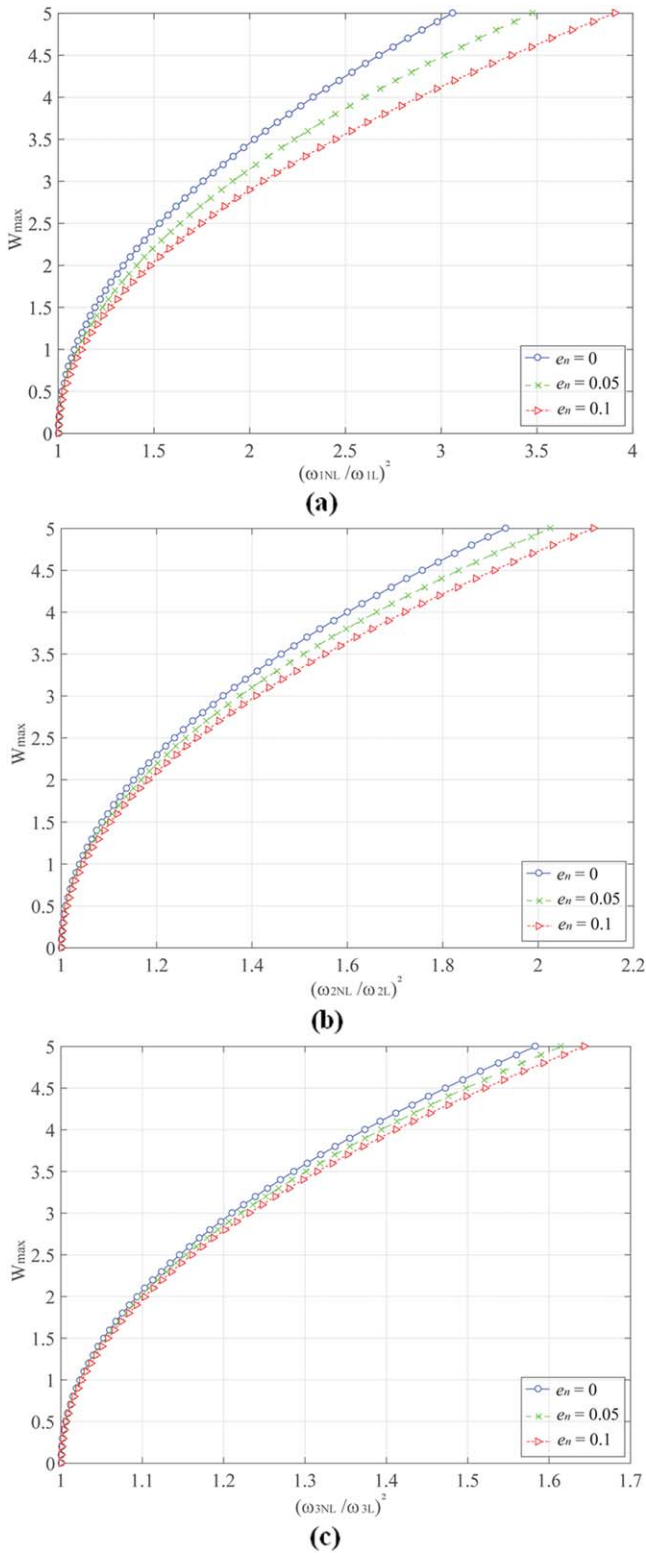


Figure 5. The effect of small-scale parameter e_n on the dimensionless nonlinear to linear frequency ratio versus the maximum initial deflection of hybrid nanotube for ($h_x = 0.05$, $\xi = 0.5$, $\Delta T = 0$, $nu = 0.3$, $Rout = 3.5e-9$, $ht = 0.34e-9$) (a) first mode (b) second mode (c) third mode.

straight beam composed of a homogeneous material compared to the results reported in the previous works. In addition, the properties of carbon and boron-nitride nanotubes

used in the simulations are tabulated in table 2. The numerical results in table 1 agrees well with those calculated by [51, 52].

4.2. Numerical analysis

The main objective of this study is to nonlinearly investigate the natural frequencies of the hetero-nanotube made of carbon and boron nitride nanotubes, we first examine the ratio of nonlinear to linear frequency for the first three vibrational modes versus the initial deflection of the system. For this purpose, figures 3–5 present the influence of key parameters on the nonlinear vibrational behavior of nonlocal hetero-nanotube. In all diagrams, the initial amplitude of the structure is considered to lie in the interval $0 < W_{max} < 5$. In the first plot to clearly explore the influence of W_{max} on the deviation of the nonlinear frequency with respect to linear one, the effects of magneto-thermal environment and size-dependency are neglected in the simulations. It is obviously revealed that the effect of initial deformation is to increase the nonlinear to linear frequency ratio and interestingly as the length ratio parameter ξ decreases, which means that the contribution of carbon part in hetero-nanotube reduces, the ratio of nonlinear to linear frequencies increases for all three vibration modes. On the other hand, by taking a deeper look into the illustrated results, it is inferred that the value of this ratio will decrease by for the higher modes of the system.

For a more in-depth investigation, figures 4(a)–(c) present the effect of temperature changes on the nonlinear natural frequency of the system neglecting the effects of magnetic field and nonlocality of nanotube when the length ratio parameter ξ is set to be 0.5. To this end, two different situations are considered. It is assumed that the system works in low and high temperature conditions in which according to the experimental results, the coefficients of thermal expansion for both carbon and boron-nitride fragments takes the negative and positive values, respectively. So, it is very important to accurately discover the behavior of the system in such different conditions. The plotted results in figures 4(a) to (c) reveal that when the hetero-nanotube works in low temperature environment, the effect of thermal gradients is to decrease the nonlinear frequency of nanotube and on the other hand, for the case of high temperature conditions, however, the nonlinear to linear frequency ratio shift upward by increasing the temperature changes. Moreover, by comparing the behavior of the first three vibration modes, one can conclude that the lower modes are more sensitive to temperature change effects.

Figure 5 exhibits the effect of nonlocal parameter of stress-driven approach on the variation of nonlinear frequency. As can be seen, for the considered three vibration modes, at higher values of nonlocal parameter e_n the hetero-nanotube becomes stiffer and the nonlinear to linear frequency ratio shifts upward as the nonlocal parameter takes the larger values. Moreover, one can clearly observe that the effect of large deformation is more dominant at lower natural frequencies. This means that the deviation of the nonlinear

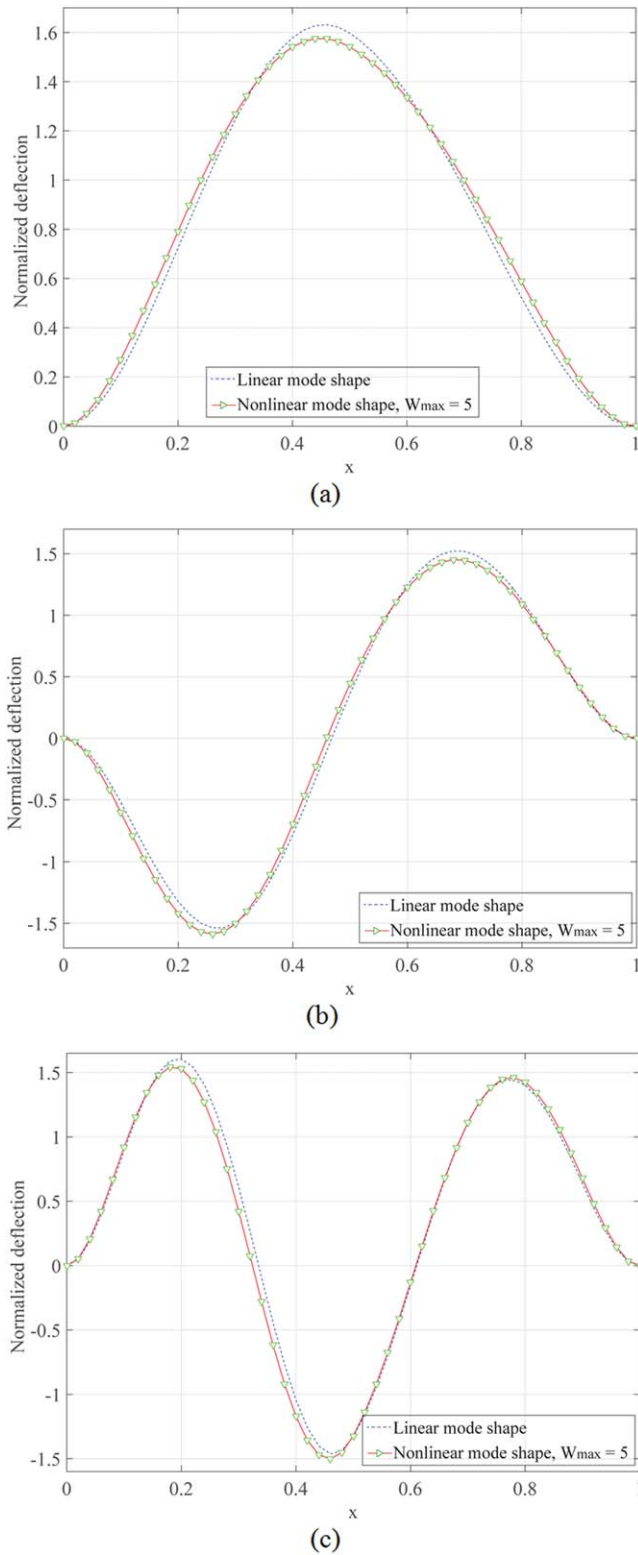


Figure 6. The effect of initial deflection on the mode shape configuration of hybrid nanotube ($h_{3x} = 0.1$, $W_{\max} = 5$, $\Delta T = 0$, $\xi = 0.5$, $e_n = 0$) (a) 1st mode (b) 2nd mode (c) 3rd mode.

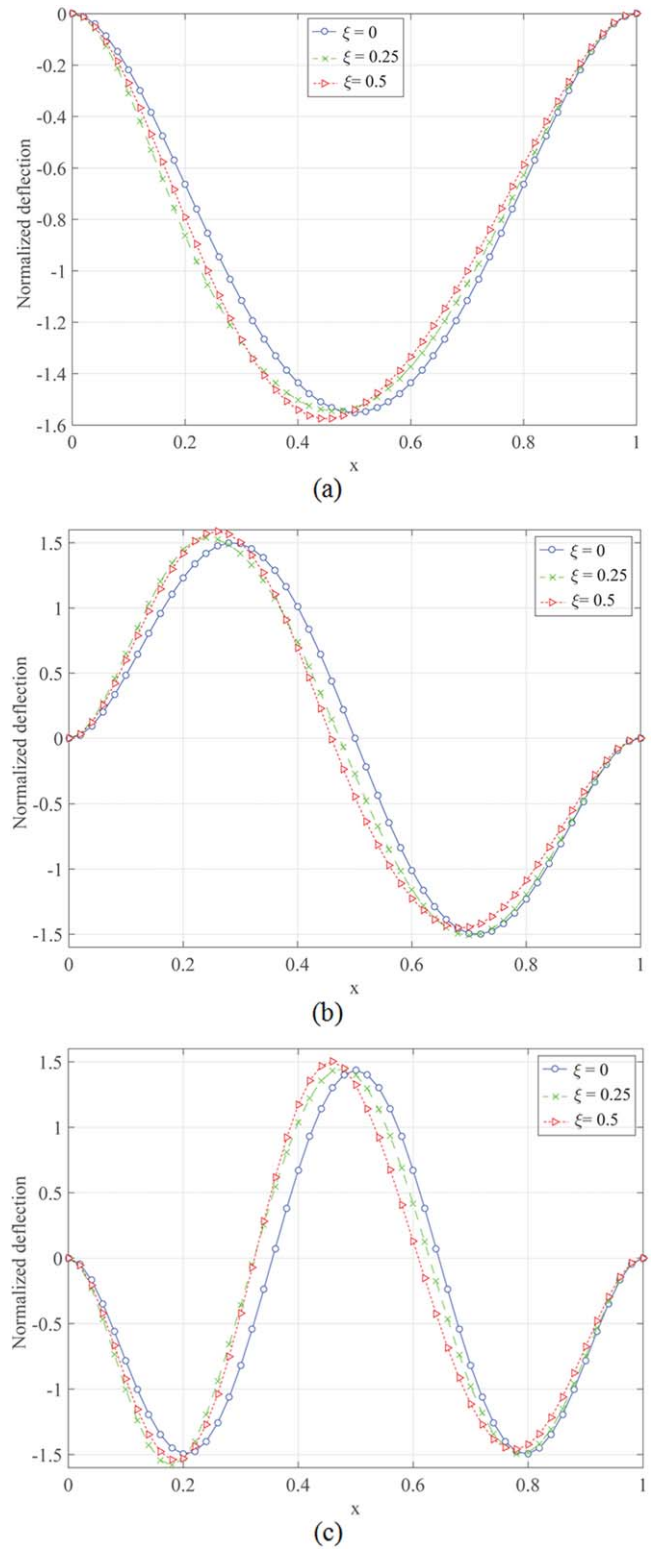


Figure 7. The effect of length ratio on the mode shape configuration of hybrid nanotube ($h_{3x} = 0.1$, $W_{\max} = 5$, $\Delta T = 0$, $\xi = 0.5$, $e_n = 0$) (a) 1st mode (b) 2nd mode (c) 3rd mode.

frequency from the linear one is meaningful at lower vibrational modes.

This discussion can be supplemented by further examination through considering the variation of nonlinear mode

shapes of vibrating hetero-nanotube as the initial amplitude is remarkable compared to the geometry of the structure. To this end, figures 6 and 7 illustrate the influence of initial amplitude and the length ratio on the configuration of the nonlinear

mode shapes of the nanotube in comparison with the linear modes. According to the presented results in figure 6, it is seen that the configuration of the first three modes may be different from those of linear modes when the initial rise of the nanotube is large enough. So, the linear mode shapes are not further valid and should not be taken into consideration in modal as well as eigen-value analyses of such structures. Figures 7(a)–(c) exhibit the influence of the variation of the length ratio on the nonlinear dynamics of the system. As previously defined, this parameter takes the values between zero and unity in which setting $\xi = 0$ indicates that the hybrid nanotube is entirely composed of boron-nitride nanotube. By taking a glance into the presented results, one can infer that as the value of the length ratio parameter increases, the location of the maximum amplitude of the first mode moves to the left end of nanotube and its impact to change the configuration of the mode shapes seems to be more considerable compared to the variation of initial rise W_{\max} . On the other hand, in the case of second and third mode shapes, by increasing the contribution of the carbon material, the location of nodes varies and shift to the left clamped edge at higher values of the length ratio parameter.

5. Concluding remarks

The impacts of the initial amplitude, length ratio, thermal gradient and size-dependency on the nonlinear vibration of a composite carbon/boron nitride hetero-nanotube were presented and discussed in the current study. A stress-driven formulation of nonlocal theory of elasticity was taken into consideration to show the size-dependent dynamics the system. The nonlinear governing equations of motion were developed by considering the von-Karman strains and discretized by means of finite element method. An eigenvalue problem was derived and the nonlinear natural frequency of the nano-hetero-structure was obtained as a function of the initial deflection. The main findings of this study can be summarized as follows:

- The deviation of the nonlinear frequency compared to the linear one is quite noticeable as the initial deflections increase.
- The variation of the maximum amplitude as well as the length ratio result in changing the location of node and the maximum deflections in the configuration of mode shapes. This variation is more sensitive to the values of the length ratio in contrast to the initial rise value.
- Temperature rise in room temperature conditions leads to decrease the natural frequencies and on the other hand, for the case of high temperature, its effect is to increase the values of the nonlinear frequencies.
- The effect of nonlocal parameter for the stress-driven approach is to increase the nonlinear frequency of the system and its effect is more considerable in lower vibration modes.

Conflict of interest

The authors declared no potential conflicts of interest with respect to the research, authorship and publication of this article.

Funding

The authors received no financial support for the research, authorship and publication of this article.

ORCID iDs

Hamid M Sedighi  <https://orcid.org/0000-0002-3852-5473>
 Mohammad Malikan  <https://orcid.org/0000-0001-7356-2168>

References

- [1] Ebrahimi N and Tadi Beni Y 2016 Electro-mechanical vibration of nanoshells using consistent size-dependent piezoelectric theory *Steel and Composite Structures* **22** 1301–36
- [2] Kheibari F and Tadi Beni Y 2017 Size dependent electro-mechanical vibration of single-walled piezoelectric nanotubes using thin shell model *Mater. Des.* **114** 572–83
- [3] Fattahian Dehkordi S and Tadi Beni Y 2017 Electro-mechanical free vibration of single-walled piezoelectric/flexoelectric nano cones using consistent couple stress theory *Int. J. Mech. Sci.* **128–129** 125–39
- [4] Soleimani S and Beni Y T 2018 Vibration analysis of nanotubes based on two-node size dependent axisymmetric shell element *Archives of Civil and Mechanical Engineering* **18** 1345–58
- [5] Dumortier H *et al* 2006 Functionalized carbon nanotubes are non-cytotoxic and preserve the functionality of primary immune cells *Nano Lett.* **6** 1522–8
- [6] Hernández-Acosta M A *et al* 2018 Fractional and chaotic electrical signatures exhibited by random carbon nanotube networks *Phys. Scr.* **93** 125801
- [7] Khosravi Y *et al* 2018 Fabrication of a novel carbon nanotube & graphene based device for gas detection *Phys. Scr.* **93** 065801
- [8] Laurila T 2015 Hybrid carbon nanomaterials for electrochemical detection of biomolecules *Phys. Scr.* **90** 094006
- [9] Karimov K S *et al* 2011 A carbon nanotube-based pressure sensor *Phys. Scr.* **83** 065703
- [10] Nozaki H and Itho S 1996 Lattice dynamics of a layered material BC₂N *Physica B* **219–2** 20 487–9
- [11] Stephan O, Ajayan P M, Colliex C, Redlich P, Lambert J M, Bernier P and Lefin P 1994 Doping graphitic and carbon nanotube structures with boron and nitrogen *Science* **266** 1683–5
- [12] Suryavanshi A P, Yu M F, Wen J, Tang C and Bando Y 2004 Elastic modulus and resonance behavior of boron nitride nanotubes *Appl. Phys. Lett.* **84** 2527–9
- [13] Chen Y, Zou J, Campbell S J and Le Caer G 2004 Boron nitride nanotubes: pronounced resistance to oxidation *Appl. Phys. Lett.* **84** 2430–2

- [14] Han W-Q, Mickelson W, Cumings J and Zettl A 2002 Transformation of Bx Cy Nz nanotubes to pure BN nanotubes *Appl. Phys. Lett.* **81** 1110
- [15] Chopra N G, Luyken R J, Cherrey K, Crespi V H, Cohen M L, Louie S G and Zettl A 1995 Boron nitride nanotubes *Science* **269** 966–7
- [16] Iijima S and Ichihashi T 1993 Single-shell carbon nanotubes of 1-nm diameter *Nature* **363** 603–5
- [17] Pumera M and Miyahara Y 2009 What amount of metallic impurities in carbon nanotubes is small enough not to dominate their redox properties? *Nanoscale* **1** 260–5
- [18] Diana S, Janet H, James W and Marisabel L-C 2012 *Hybrid Boron Nitride Nanotubes—Carbon Nanostructures Supercapacitor with High Energy Density* E-663225 (Washington, DC, United States: NASA Headquarters)
- [19] Rodríguez Juárez A, Anota C, Hernández Cocolletzi H, Sánchez Ramírez J F and Castro M 2017 Stability and electronic properties of armchair boron nitride/carbon nanotubes *Fullerenes, Nanotubes and Carbon Nanostructures* **25** 716–25
- [20] Xiao H, Zhang C X, Zhang K W, Sun L Z and Zhong J X 2013 Tunable differential conductance of single wall C/BN nanotube heterostructure *J. Mol. Model.* **19** 2965–9
- [21] Zhang J and Wang C Y 2017 Beat vibration of hybrid boron nitride-carbon nanotubes—a new avenue to atomicscale mass sensing *Comput. Mater. Sci.* **127** 270–6
- [22] Vedaei S S and Nadimi E 2019 Gas sensing properties of CNT-BNNT-CNT nanostructures: a first principles study *Appl. Surf. Sci.* **470** 933–42
- [23] Chen X K, Xie Z X, Zhang Y, Deng Y X, Zou T H, Liu J and Chen K Q 2019 Highly efficient thermal rectification in carbon/boron nitride Heteronanotubes *Carbon* **148** 532–9
- [24] Badjian H and Setoodeh A R 2017 Improved tensile and buckling behavior of defected carbon nanotubes utilizing boron nitride coating—a molecular dynamics study *Physica B* **507** 156–63
- [25] Genoese A, Genoese A and Salerno G 2019 On the nanoscale behaviour of single-wall C, BN and SiC nanotubes *Acta Mech.* (<https://doi.org/10.1007/s00707-018-2336-7>)
- [26] Eltahir M A, Almalki T A, Almitani K H, Ahmed K I E and Abdraboh A M 2019 Modal participation of fixed–fixed single-walled carbon nanotube with vacancies *International Journal of Advanced Structural Engineering* **11** 151–63
- [27] Kiani K and Pakdaman H 2020 On the nonlocality of bilateral vibrations of single-layered membranes from vertically aligned double-walled carbon nanotubes *Phys. Scr.* **95** 035221
- [28] Salamat D and Sedighi H M 2017 The effect of small scale on the vibrational behavior of single-walled carbon nanotubes with a moving nanoparticle *Journal of Applied and Computational Mechanics* **3** 208–17
- [29] Sedighi H M and Yaghootian A 2016 Dynamic instability of vibrating carbon nanotubes near small layers of graphite sheets based on nonlocal continuum elasticity *J. Appl. Mech. Tech. Phys.* **57** 90–100
- [30] Choyal V K, Choyal V, Nevhal S, Bergaley A and Kundalwal S I 2019 Effect of aspects ratio on Young's modulus of boron nitride nanotubes: a molecular dynamics study *Materials Today: Proceedings* (<https://doi.org/10.1016/j.matpr.2019.05.347>)
- [31] Ramezannejad Azarboni H 2019 Magneto-thermal primary frequency response analysis of carbon nanotube considering surface effect under different boundary conditions *Composites Part B: Engineering* **165** 435–41
- [32] Karami B and Janghorban M 2019 On the dynamics of porous nanotubes with variable material properties and variable thickness *Int. J. Eng. Sci.* **136** 53–66
- [33] Zhu B, Chen X, Dong Y and Li Y 2019 Stability analysis of cantilever carbon nanotubes subjected to partially distributed tangential force and viscoelastic foundation *Appl. Math. Modell.* **73** 190–209
- [34] Hołubowski R, Glabisz W and Jarczewska K 2019 Transverse vibration analysis of a single-walled carbon nanotube under a random load action *Physica E* **109** 242–7
- [35] Zhen Y-X, Wen S-L and Tang Y 2019 Free vibration analysis of viscoelastic nanotubes under longitudinal magnetic field based on nonlocal strain gradient Timoshenko beam model *Physica E* **105** 116–24
- [36] Narendar S, Gupta S S and Gopalakrishnan S 2012 Wave propagation in single-walled carbon nanotube under longitudinal magnetic field using nonlocal Euler–Bernoulli beam theory *Appl. Math. Modell.* **36** 4529–38
- [37] Romano G and Barretta R 2017 Nonlocal elasticity in nanobeams: the stress-driven integral model *Int. J. Eng. Sci.* **115** 14–27
- [38] Barretta R *et al* 2018 Exact solutions of inflected functionally graded nano-beams in integral elasticity *Composites Part B: Engineering* **142** 273–86
- [39] Barretta R *et al* 2018 Closed-form solutions in stress-driven two-phase integral elasticity for bending of functionally graded nano-beams *Physica E* **97** 13–30
- [40] Wang L, Ni Q, Li M and Qia Q 2008 The thermal effect on vibration and instability of carbon nanotubes conveying fluid *Physica E* **40** 3179–82
- [41] Numanoğlu H M, Akgöz B and Civalek O 2018 On dynamic analysis of nanorods *Int. J. Eng. Sci.* **130** 33–50
- [42] Demir C and Civalek O 2017 On the analysis of microbeams *Int. J. Eng. Sci.* **121** 14–33
- [43] Civalek O and Demir C 2011 Buckling and bending analyses of cantilever carbon nanotubes using the Euler–Bernoulli beam theory based on non-local continuum model *Asian Journal of Civil Engineering* **12** 651–61
- [44] Civalek O and Demir C 2011 Bending analysis of microtubules using nonlocal Euler–Bernoulli beam theory *Appl. Math. Modell.* **35** 2053–67
- [45] Li L, Hu Y and Li X 2016 Longitudinal vibration of size-dependent rods via nonlocal strain gradient theory *Int. J. Mech. Sci.* **115–1** 16 135–44
- [46] Barretta R, Faghidian S A and Luciano R 2019 Longitudinal vibrations of nano-rods by stress-driven integral elasticity *Mech. Adv. Mater. Struct.* **26** 1307–15
- [47] Barretta R, Caporale A, Faghidian S A, Luciano R, Marotti de Sciarra F and Medaglia C M 2019 A stress-driven local-nonlocal mixture model for Timoshenko nano-beams *Composites Part B: Engineering* **164** 590–8
- [48] Barretta R and Marotti de Sciarra F 2019 Axial and flexional behaviour of elastic nano-beams by stress-driven two-phase elasticity *Advances in Engineering Materials, Structures and Systems: Innovations, Mechanics and Applications—Proc. of the 7th Int. Conf. on Structural Engineering, Mechanics and Computation* 486–91
- [49] Barretta R, Fabbrocino F, Luciano R, de Sciarra F M and Ruta G 2019 Buckling loads of nano-beams in stress-driven nonlocal elasticity *Mech. Adv. Mater. Struct.* (<https://doi.org/10.1080/15376494.2018.1501523>)
- [50] Barretta R, Faghidian S A, Luciano R, Medaglia C M and Penna R 2018 Free vibrations of FG elastic Timoshenko nano-beams by strain gradient and stress-driven nonlocal models *Composites Part B: Engineering* **154** 20–32
- [51] BHashyam G R and Prathap G 1980 Galerkin finite element method for nonlinear beam vibrations *J. Sound Vib.* **72** 191–203
- [52] Evensen D A 1968 Nonlinear vibrations of beams with various boundary conditions *AIAA J.* **6** 370–2
- [53] Cheng Q, Liu Y S, Wang G C, Liu H, Jin M G and Li R 2019 Free vibration of a fluid-conveying nanotube constructed by carbon nanotube and boron nitride nanotube *Physica E* **109** 183–90